Quantification of the pore occurrence by 2D/3D image analysis and S-wave velocity prediction by the Differential Effective Medium theory in Albian grainstones

Irineu A. Lima Neto[1], Roseane M. Misságia[1,2], Marco A. R. Ceia[1,2], Carolina P. Gonçalves[1] and Nathaly L. Archilha[3]
[1]LENEP –UENF; [2]INCT-GP; [3]LNLS-IMX

This paper was prepared for presentation during the 15th International Congress of the Brazilian Geophysical Society held in Rio de Janeiro, Brazil, 31 July to 3 August, 2017.

Abstract

Carbonates hold the main oil and gas reservoirs at worldwide. In Brazil, carbonates are present in pre- and post-salt deposits. The digenetic heterogeneity observed in carbonates may cause a low hydrocarbon recovery. Therefore, carbonate studies are necessary, especially to correlate mineralogy, texture and elastic properties and predict rock physics models suitable to support hydrocarbon recovery. The data set of this study treats 6 cored Albian oncolitic/oolitic grainstone samples from a reservoir interval in Campos basin – Brazil. Petrophysical measurements as porosity, permeability and mineralogy are available. Thin section images and a recent acquisition of tomography data volume allow us to employ digital image analysis, quantify macro-meso and micropore inclusions and promote discussions for data processing and differences between image resolutions. A method based on Differential Effective Medium theory is applied to invert the microporosity aspect ratio (geometrical pore parameter) and correlate elastic properties with macro-meso and micropore inclusions to predict S-wave velocity at minimum error by measured P-wave velocity. Discussions about pore geometry of inclusions, elastic moduli and velocities are performed by the digital image analysis perspective.

Introduction

Carbonate rocks have a wide economic significance around the world and hold more than 50% of the oil and gas reserves (e.g., Burchette, 2012). These rocks are present in Brazilian reservoirs and the importance has improved with new discoveries in the post- and pre-salt oil deposits (Bruhn et al., 2003).

Heterogeneities are commonly observed in carbonates due to chemical reactions during diagenesis and exhibit complicated mineral composition, pore structure and texture anomalies that may cause a low hydrocarbon recovery (e.g., Anselmetti & Eberli, 1993; Anselmetti et al., 1998). Thus, the relationship between reservoir rocks and elastic properties is important to understanding and improving the practical rock physics models.

Petrophysics studies can determine porosity and permeability of rocks in laboratory. Texture complexities are widely characterized by digital image analysis, employing different methods as petrographic thin sections and tomography images. For example, textural characterization performed by image analysis is especially able to characterize macro-mesopores. Generally, micropores are underestimated by image analysis due to resolution limitations (e.g., Anselmetti & Eberli, 1993; Assefa et al., 2003; Eberli et al., 2003; Kumar and Han, 2005; Weger et al., 2009). Thereby, a study method is necessary to characterize micropores that may occur in carbonate rocks and correlate them with other textural, mineralogical and elastic parameters in order to predict P- and S-wave velocities.

This study improves the knowledge about oncolitic/oolitic grainstones from Campos basin by the digital image analysis to support the textural correlation with the mineralogical and elastic properties of rocks at laboratory scale.

Data set

This study treats laboratory measurements of 6 limestone samples from a cored well in Campos basin, southeastern Brazil, early to middle Albian age, captured from a reservoir interval. The carbonate shelf was originated from cycles of upward shoaling lithological sequences that started with peloidal wackestones, followed by oncolitic/oolitic packstones and oncolitic/oolitic grainstones, deposited in a lower energy environment (Bruhn et al., 2003). All available samples exhibit oncolitic/oolitic grainstone texture with good porosity (~24.8%) and permeability (~4 – 222 mD) conditions, estimated by Archilha et al. (2013) – Tab. 1.

Quantitative mineralogy analyses were performed using XRD (X-ray diffraction) and Rietveld method and the results showed calcite as the predominant mineral. The elastic bulk (K) and shear (μ) moduli of the mineral matrix were predicted by Voigt-Reuss-Hill average method using the XRD information (see Archilha et al., 2013; Lima Neto et al., 2013, 2014) – summarized in Tab. 1.

Ultrasonic P- and S-wave measurements were performed in room dried samples at effective pressure of ~5 MPa, using the pulse transmission method at approximately 1.3 MHz and 900 KHz, respectively (Lima Neto et al., 2014,

2015). Velocities (Vp and Vs) were computed as shown in Tab. 1.

Table 1 *– Data set and laboratory measurements. P- and S-wave velocities (Vp and Vs, respectively) were estimated using the pulse transmission method at room dried samples and effective pressure of ~5 MPa. Bulk and shear moduli and density of matrix were computed after mineralogy analyses.*

Sample	Vp (km/s)	Vs (km/s)	K_0 (GPa)	μ_0 (GPa)	ρ_0 (GPa)
W1-Im1	3.378	1.922	71.06	30.04	2.71
W1-Im2	3.158	1.868	69.32	29.97	2.71
W1-Im3	3.115	1.868	70.75	30.15	2.71
W1-Im4	3.527	2.101	69.66	29.89	2.71
W1-Im5	2.135	1.475	70.96	30.50	2.72
W1-Im6	3.095	1.837	70.60	30.22	2.71

Table 2 *– Digital image analysis properties.*

Nature of image	Optical Microscopy	X-ray microCT
Pixel (or voxel) resolution (µm)	4.04 (25X)	1.64 (5X)
Minimum pixel quantity in diameter	2	4
Pore area resolution (µm²)	~65.29	43.04
Representativeness of data volume	thin sections of 764 x 540 pixels (2D)	~450 x 500 x 600 pixels (3D)
Threshold calibration	Automatic blue scale and visual validation by an interpreter	Otsu's method (mainly)

Petrographic thin section (2D) and microtomography scan (microCT 3D) analyses were performed in previous studies (Archilha et al., 2013, 2014, 2016; Lima Neto et al., 2013, 2014, 2015). However, the petrographic images were reprocessed in this study using Fiji-ImageJ and JPOR macro toolset (open source software) to quantify total optical porosity from blue stained thin sections (Grove & Jerram, 2011). New microCT scans were performed at Brazilian Synchrotron Light Laboratory – IMX (X-ray Imaging) beamline and facilities at CNPEM (Brazilian Research Center in Materials and Energy area). The data volume was reconstructed and converted to 8-bits gray scale. Additionally, we picked the volume of interest from data for analysis and segmentation avoiding rings originated from border-scattering. The Otsu's method (Otsu, 1979) was applied as an automatic procedure for threshold analysis and supported by a visual validation interpreter and pores were computed using the PoreShape GeoLab routines of licensed software GeoDict 2015. Tab. 2 and Fig. 1 summarize the digital image analysis properties. Pore properties were computed as aspect ratio (a local parameter that describes the elongation of the pore-bounding ellipsoid, estimated by the ratio between the major and minor semi-axes, approximated to oblate spheroids) and quantity of macro-meso and micropores.

Digital image analysis of images and petrophysical measurements aim to characterize the rock specimen, highlighting mineralogy, texture and elastic properties of carbonates. Those properties are important to employ the study method.

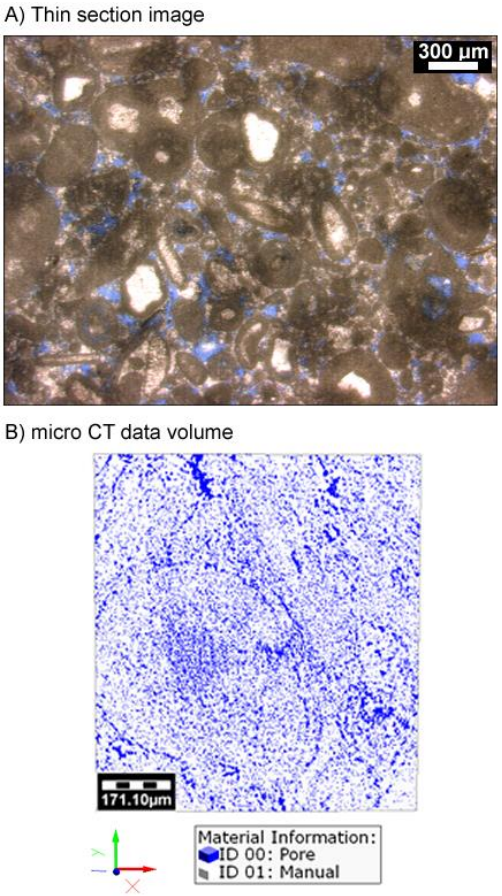

Figure 1 *– Brief comparison between images from (A) Optical microscopy of blue stained thin section and (B) microCT data volume (pore in blue), an example of specimen W1-Im4 (*oncolitic/oolitic grainstone*).*

Methodology and Results

The study method is summarized in Fig. 2. As stated by Lima Neto et al. (2014), the Differential Effective Medium (DEM) theory (Berryman, 1992) is applied to determine K and µ moduli of dry rock using macro-meso and micropore information as inclusions. Therefore, the micropore aspect ratio (α) is assumed at minimum error between measured and calculated Vp. After that, Vs can

be calculated using the calibrated shear modulus for inclusions and compared with measurements.

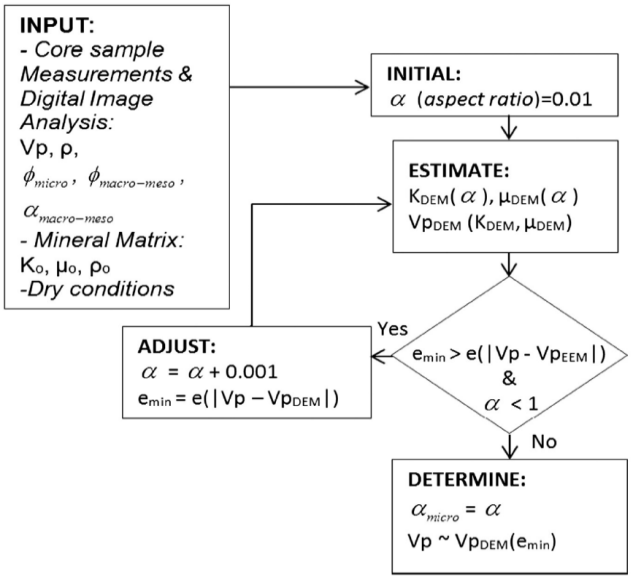

Figure 2 *- Rock Physics method to predict the microporosity aspect ratio and promote elastic properties correlation (Lima Neto et al., 2014).*

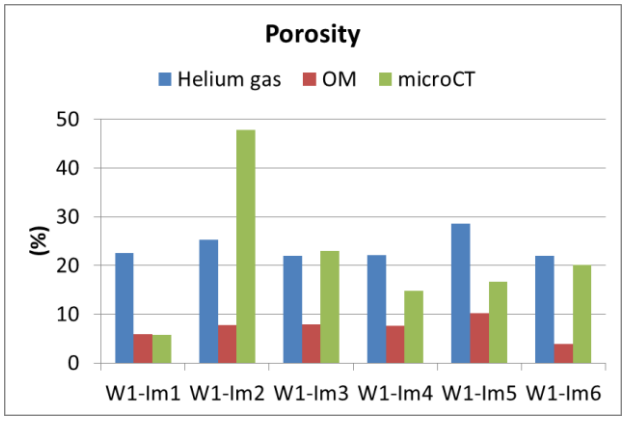

Figure 3 *– Porosity estimation: (1) helium gas laboratory measurements; image porosity computed from (2) OM (optical microscopy thin sections – 2D) and (3) microCT (3D).*

The macro-mesopores generally can be detected by different imaging techniques. However, microporosity detection is critical for complex rocks as carbonates, especially due to the image resolution limitations. Two imaging techniques were performed as shown in Tab. 2 and Fig. 1, thin section images from optical microscopy (OM) display lower resolution than the microCT data volume, and it was the motivation to keep the minimum pixel quantity of 2 in diameter to represent the pore space. On the other hand, a minimum quantity of 4 pixels in diameter was considered during microCT data analysis to detect pores and this approach tends to produce more representative results of pore geometry properties as aspect ratio (as discussed by Weger, 2006). Pore aspect ratio is a 2D parameter, thus aspect ratio of 3D pores were computed by the X- and Y-elongations. In addition, resolution limitations can cause an image porosity underestimation as identified in this study for thin section images (Fig. 3). Pore aspect ratio was computed for each sample and results are showed in Fig. 4.

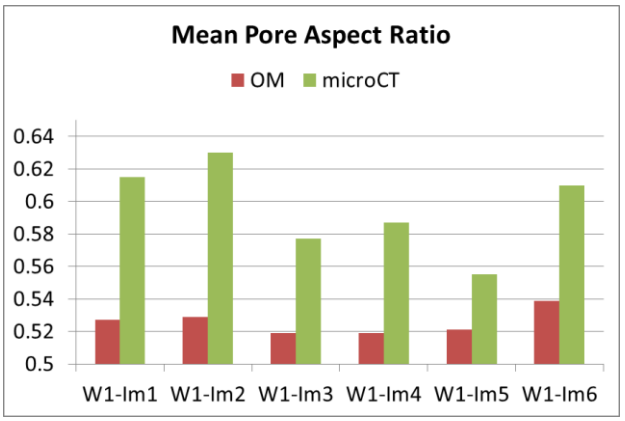

Figure 4 *– Mean (average) pore aspect ratio results from image analyses: OM (optical microscopy thin sections – 2D) and microCT (3D).*

Approach differences from image analyses suggest discrepancy of image porosity results (Fig. 3). As consequence, porosity estimated by optical microscopy tends to be lower than the helium gas. Although that, image porosities estimated using microCT data volume showed similar tendency values for most of all samples. In some cases, image porosity is higher than the helium gas porosity and these probably express a low representativeness of images to characterize the plug samples, taking account the expected higher results of helium gas that is able to fill the whole pore system, including micropores that may are not detected by images due to resolution limitations. Therefore, quantify micropores in carbonates is a common trouble employing digital image analysis. Some assumptions were done to classify porosity occurrence in macro-meso and micropores (as necessary for the inclusion method in Fig. 2), which are based on laboratory porosity measurements and image pore classification in literature as proposed by Anselmetti et al. (1998) (macro-mesopore area ≥ 500 μm² - commonly applied for carbonates). Two suppositions were tested:

A) Thin section images from OM: micropores were estimated by the difference between helium gas (bulk) and detected image (macro-meso) porosities;

B) MicroCT data: detected pores were classified by Anselmetti et al. (1998) to determine the relative occurrence of macro-mesopores and micropores (area < 500 μm²). Pores that may be not recognized under the microCT resolution were

ignored by the supposition to express low significance in oncolitic/oolitic grainstones if compared to the representativeness of the whole rock sample in up/downscaling.

Figure 5 shows the Anselmetti et al. (1998)'s classification results applied to OM images and the low efficiency to characterize micropores. The same classification was extended to microCT data (Fig. 6) and assumed suitable to quantify macro-meso and micropores during the digital image analysis.

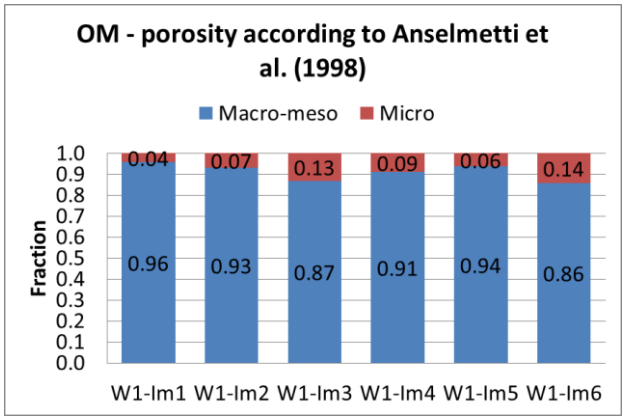

***Figure 5** – Digital image analysis of thin sections (OM) showed low micropore occurrence according to the Anselmetti et al. (1998)'s classification (pore area lower than 500 µm²), suggesting that the method is able to detect macro-mesopores due to resolution limitations.*

Finally, microporosity aspect ratio was computed for suppositions A and B by the method in Fig. 2, using the inherent input properties for each assumption case as macro-meso and micropore quantity, and macro-mesopore aspect ratio, which were computed by digital image analyses. The K and µ moduli were computed using DEM Rock Physics model at a minimum error of Vp, allowing to predict the microporosity aspect ratio and results are displayed in Tab. 3.

The efficiency of the method can be verified by the fit between measured and predicted velocities given by Eq. 1:

$$R = 1 - \frac{|\text{Vmeasured} - \text{Vpredicted}|}{\text{Vmeasured}}. \quad (1)$$

Therefore, Figs. 7 and 8 show the fit efficiency of Vp and Vs for each supposition A and B, respectively. Vp fit results displayed R = ~1 for both suppositions and confirm that the macro-meso and microporosity were appropriated established for each image resolution, allowing us to apply satisfactorily the same method in Fig. 2. This result is particularly interesting for digital image approaches that use different method resolutions. An extra test was performed using the thin section images (OM) and the macro-meso and micropores classified by Anselmetti et al. (1998), displayed in Fig 5, and the method (Fig. 2) resulted in the worst fit of velocities (R < 0.8). It was expected by the underestimation of microporosity that is more pronounced in modeling that the observed differences in macro-mesopore aspect ratio from MO and microCT, showed in Fig. 4.

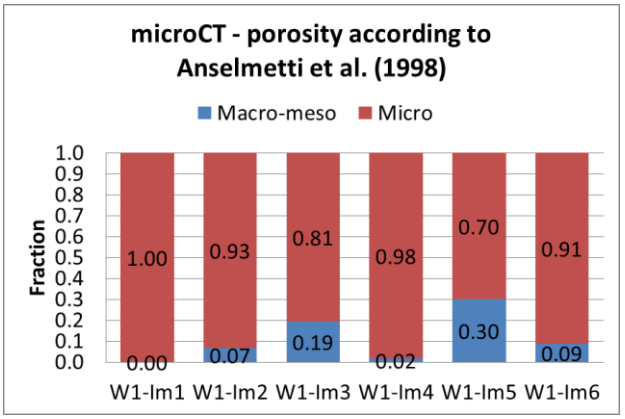

***Figure 6** – Digital image analysis of microCT data – results showed high micropore occurrence (pore area lower than 500 µm²), and the Anselmetti et al. (1998)'s classification was adopted in this case to quantify macro-meso and micropores.*

Vs was predicted and compared with the measurements in Figs. 7 and 8 - B. Coincidently, the general fit results were the same for both suppositions A and B (R = 0.925), although the observed slight fit scattering on Vs prediction of samples. This result showed that the method and assumptions are suitable for Vs prediction by Vp measurements and modeling by the pore system characterization using digital image analysis.

Conclusions

New image acquisitions and the performed digital analysis improved the knowledge about the oncolitic/oolitic grainstones in data set. The microCT data gave us a more accurate sense of pore occurrences, classified as macro-meso and micropores, according to Anselmetti et al. (1998) approach. Moreover, thin section images were reprocessed and although the resolution limitation expressed a microporosity underestimation, results showed that the images contributed to the characterization of macro-mesopores. In addition, micropores may be computed by the bulk porosity difference as treated in this study, through the difference between helium gas and optical image porosities. The modeling method revealed that differences between pore inclusion assumptions for porosity quantification seem to

be more expressive than the differences between the pore aspect ratio.

Microporosity aspect ratio (α) was determined successfully by the method, allowing K and μ moduli estimation of dry rock. The inverted microporosity aspect ratio results (Tab. 3) for assumptions using the thin section image analysis from Optical Microscopy (OM) and microCT data are approximately equal, expressing $\alpha \leq \sim 1$, although the assumed differences for the pore quantification.

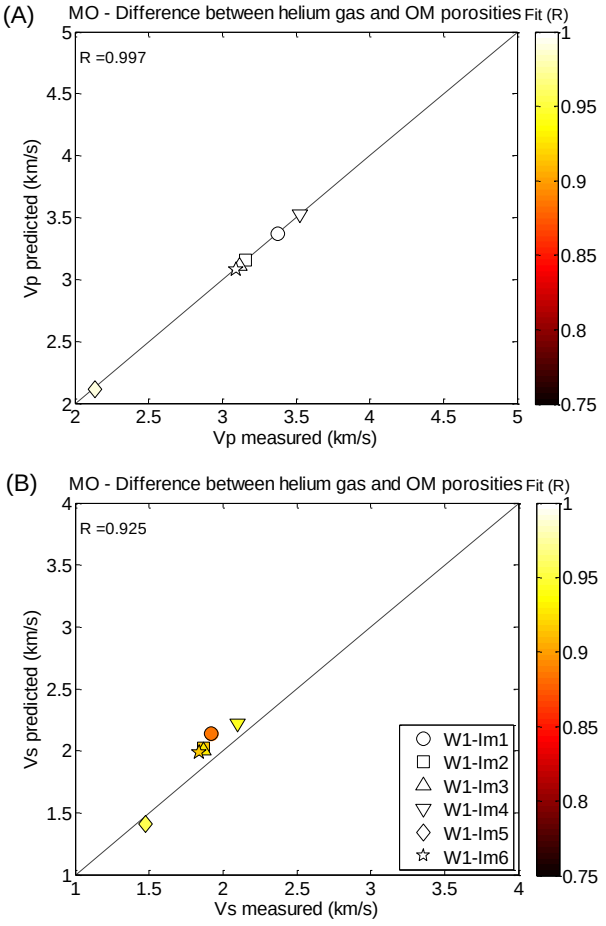

Figure 7 *– Modeling velocity results for the supposition (A): macro-mesopores determined by the thin section images and micropores by the difference between helium gas and optical microscopy (OM) porosities.*

The general fit results of modeling were reached satisfactorily using Vp measurement ($R \approx 1$). After that, the calibrated μ modulus was employed to compute Vs and compared with measurements, expressing satisfactory general fit results ($R \approx 0.925$) for all supposition cases of pore inclusions.

As discussed, microporosity quantification is a common trouble in digital image analysis of rocks and differences in method resolutions cause result discrepancy and determining the best approach for each case is not an easy task. The discussions in this work were performed for granular rocks that exhibit predominant intergranular porosity. Rocks with matrix supported by mud as dolostones tend to present high microporosity occurrence (microporous matrix), increasing the difficulties to quantify pores by the image analysis.

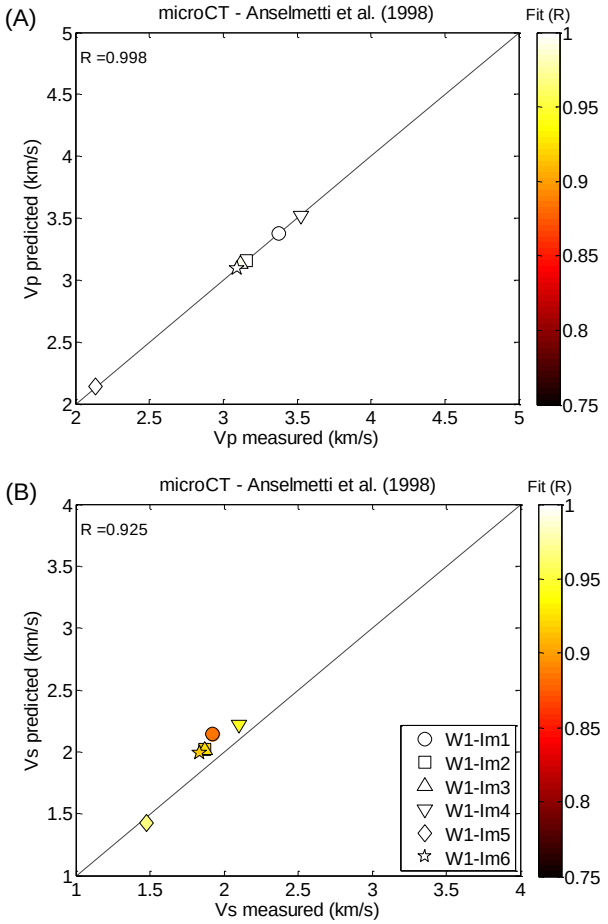

Figure 8 *- Modeling velocity results for the supposition (B):* detected pores were classified by Anselmetti et al. (1998) to determine the relative occurrence of macro-meso and micropores.

Table 3 *– Microporosity aspect ratio results after method application for two suppositions: A) thin section image analysis from Optical Microscopy (OM); B) microCT data. Both results are consistent to characterize micropores that generally exhibit low aspect ratio (< ~0.1).*

Sample	Supposition (A)	Supposition (B)
W1-Im1	0.0810	0.1080
W1-Im2	0.0770	0.1020
W1-Im3	0.0590	0.0740
W1-Im4	0.0780	0.1130
W1-Im5	0.0470	0.0520
W1-Im6	0.0740	0.0820

Acknowledgments

The authors would like to thank UENF/LENEP, INCT-GP, PRH-ANP-20, PRHPETROBRAS-226 and PETROBRAS for the facilities provided to perform this work. Special thanks to LNLS-IMX for all support during tomography acquisition procedures and facilities.

References

Anselmetti, F.S., Eberli, G.P., 1993. Controls on sonic velocity in carbonates. Pure and Applied Geophysics, 141, 287–323. doi: 10.1007/BF00998333.

Anselmetti, F.S., Luthi, S., Eberli, G.P., 1998. Quantitative characterization of carbonate pore systems by digital image analysis. AAPG Bulletin, 82, 1815-1836.

Archilha, N., Missagia, R., Ceia, M., Lima Neto, I., Castro, L., Souza, F., 2013. Petrophysical, mineralogical and P-wave velocity characterization of Albian carbonates from Campos Basin, Brazil. SEG Technical Program Expanded Abstracts, 2989–2993. doi: 10.1190/segam2013-0676.1.

Archilha, N.L., Missagia, R.M., Hollis, C., Ceia, M.A.R., Lima Neto, I.A., McDonald, S. A., 2014. Key controlling factors of permeability estimated from micro-CT images of Brazilian analogous pre-salt carbonate rock. SEG Technical Program Expanded Abstracts, 2703-2708. doi: 10.1190/segam2014-1284.1.

Archilha, N.L., Missagia, R.M., Hollis, C., Ceia, M.A.R., McDonald, S.A., Lima Neto, I.A., 2016. Permeability and acoustic velocity controlling factors determined from x-ray tomography images of carbonate rocks. AAPG Bulletin, 100, n. 8, 1289-1309. doi: 10.1306/02251615044.

Assefa, S., McCann, C., Sothcott, J., 2003. Velocities of compressional and shear waves in limestones. Geophysical Prospecting, 51, 1–13. doi: 10.1046/j.1365-2478.2003.00349.x.

Berryman, J.G., 1992. Single-scattering approximations for coefficients in Biot's equations of poroelasticity. The Journal of the Acoustical Society of America, 91, 551–571. doi: 10.1121/1.402518.

Bruhn, C.H., Gomes, J.A., Lucchese Jr., C.D., Johann, P.R., 2003. Campos basin: reservoir characterization and management — historical overview and future challenges. Offshore Technology Conference, OTC 15220, Houston, Texas, 1–14. doi: 10.4043/15220-MS.

Burchette, T.P, 2012. Carbonate rocks and petroleum reservoirs: a geological perspective from the industry. Geological Society, London, Special Publications, 370, 17–37. doi: 10.1144/SP370.14.

Grove, C., Jerram. D.A., 2011. JPOR: An ImageJ macro to quantify total optical porosity from blue-stained thin sections. Computers & Geosciences, 37, Issue 11, 1850-1859. doi:10.1016/j.cageo.2011.03.002.

Eberli, G.P., Baechle, G.T., Anselmetti, F.S., Incze, M.L., Dong, W., Tura, A., Sparkman, G., 2003. Factors controlling elastic properties in carbonate sediments and rocks. The Leading Edge, 22, 654–660. doi: 10.1190/1.1599691.

Kumar, M., Han, D.H., 2005. Pore shape effect on elastic properties of carbonate rocks. SEG Technical Program Expanded Abstracts, 1477–1480. doi: 10.1190/1.2147969.

Lima Neto, I., Missagia, R.M., Ceia, M.A.R., Archilha, N.L., Oliveira, L., 2013. Dual pore system evaluation of Albian grainstone carbonates from Brazil using effective elastic media theory models. SEG Technical Program Expanded Abstracts, 2994-2998. doi: 10.1190/segam2013-0652.1.

Lima Neto, I., Missagia, R.M., Ceia, M.A.R., Archilha, N.L., Oliveira, L., 2014. Carbonate pore system evaluation using the velocity-porosity–pressure relationship, digital image analysis, and differential effective medium theory. Elsevier, Journal of Applied Geophysics, 110, 23-33. doi:10.1016/j.jappgeo.2014.08.013.

Lima Neto, I., Missagia, R.M., Ceia, M.A.R., Archilha, N.L., Hollis, C., 2015. Evaluation of carbonate pore system under texture control for prediction of microporosity aspect ratio and shear wave velocity. Sedimentary Geology, 323, 43–65. doi:10.1016/j.sedgeo.2015.04.011.

Otsu, N., 1979. A threshold selection method from gray-level histograms. IEEE Trans. Sys., Man., Cyber. 9 (1), 62–66. doi:10.1109/TSMC.1979.4310076

Weger, R.J., 2006. Quantitative pore/rock type parameters in carbonates and their relationship to velocity deviations. PhD. dissertation thesis, University of Miami, Coral Glabes, 232 p.

Weger, R.J., Eberli, G.P., Baechle, G.T., Massaferro, J.L., Sun, Y., 2009. Quantification of pore structure and its effect on sonic velocity and permeability in carbonates. AAPG Bulletin, 93, 1297-1317. doi:10.1306/05270909001.